AGU PUBLICATIONS

Global Biogeochemical Cycles

RESEARCH ARTICLE
10.1002/2015GB005194

Key Points:
- Diazotrophs fix N_2 in waters with relatively elevated NO_3^- or NH_4^+ assimilation rates
- N_2 fixation, a source of N in the eastern Indian Ocean
- Conceptual understanding of how N_2 fixation products can be oxidized to NO_3^-

Supporting Information:
- Texts S1–S6, Table S1, and Figures S1–S6
- Figure S1
- Figure S2
- Figure S3
- Figure S4
- Figure S5
- Figure S6

Correspondence to:
E. J. Raes,
eric.raes@research.uwa.edu.au

Citation:
Raes, E. J., P. A. Thompson, A. S. McInnes, H. M. Nguyen, N. Hardman-Mountford, and A. M. Waite (2015), Sources of new nitrogen in the Indian Ocean, *Global Biogeochem. Cycles*, *29*, doi:10.1002/2015GB005194.

Received 24 MAY 2015
Accepted 23 JUL 2015
Accepted article online 28 JUL 2015

Sources of new nitrogen in the Indian Ocean

Eric J. Raes[1], Peter A. Thompson[2], Allison S. McInnes[3], Hoang Minh Nguyen[1], Nick Hardman-Mountford[1,4], and Anya M. Waite[5]

[1]The UWA Oceans Institute, University of Western Australia, Crawley, Western Australia, Australia, [2]CSIRO Oceans and Atmosphere Flagship, Hobart, Tasmania, Australia, [3]Plant Functional Biology and Climate Change, University of Technology, Sydney, Sydney, New South Wales, Australia, [4]CSIRO Oceans and Atmosphere Flagship, Wembley, Western Australia, Australia, [5]Alfred Wegener Institute for Polar and Marine Research, Bremerhaven and Universität Bremen, Bremen, Germany

Abstract Quantifying the different sources of nitrogen (N) within the N cycle is crucial to gain insights in oceanic phytoplankton production. To understand the controls of primary productivity and the associated capture of CO_2 through photosynthesis in the southeastern Indian Ocean, we compiled the physical and biogeochemical data from four voyages conducted in 2010, 2011, 2012, and 2013. Overall, higher NH_4^+ assimilation rates (~530 μmol m^{-2} h^{-1}) relative to NO_3^- assimilation rates (~375 μmol m^{-2} h^{-1}) suggest that the assimilation dynamics of C are primarily regulated by microbial regeneration in our region. N_2 fixation rates did not decline when other source of dissolved inorganic nitrogen were available, although the assimilation of N_2 is a highly energetic process. Our data showed that the diazotrophic community assimilated ~2 nmol N L^{-1} h^{-1} at relative elevated NH_4^+ assimilation rates ~12 nmol L^{-1} h^{-1} and NO_3^- assimilation rates ~6 nmol L^{-1} h^{-1}. The small diffusive deep water NO_3^- fluxes could not support the measured NO_3^- assimilation rates and consequently point toward another source of dissolved inorganic NO_3^-. Highest NO_2^- values coincided consistently with shallow lower dissolved O_2 layers (100–200 m; 100–180 μmol L^{-1}). These results suggest that nitrification above the pycnocline could be a significant component of the N cycle in the eastern Indian Ocean. In our analysis we provide a conceptual understanding of how NO_3^- in the photic zone could be derived from new N through N_2 fixation. We conclude with the hypothesis that N injected through N_2 fixation can be recycled within the photic zone as NH_4^+ and sequentially oxidized to NO_2^- and NO_3^- in shallow lower dissolved oxygen layers.

1. Introduction

The supply of biologically available nitrogen (N) can be a bottleneck in the efficiency of the biological oceanic carbon pump. Nitrogen budgets in the open ocean regulate primary productivity and the associated fixation of C through photosynthesis [*Ward et al.*, 2013]. The biological pump (sum of all the biologically mediated processes that export carbon) and the solubility pump (dissolution of CO_2 and its physical transport) are estimated to contribute equally to the CO_2 flux in the South Indian Ocean region [*Valsala et al.*, 2012]. However, the regulation of the biological pump by the N cycle remains enigmatic despite the urgent need to understand productivity controls in the Indian Ocean [*Alexander et al.*, 2012]. An understanding of potential alterations at the base of the food chain particularly reductions in planktonic biomass is essential, as a decline [*Boyce et al.*, 2010] or a community shift [*Montes-Hugo et al.*, 2009] in primary productivity will impact ecosystem services, such as O_2 production, carbon sequestration, biogeochemical cycling, and fisheries [*Lehodey et al.*, 2010; *Hollowed et al.*, 2013; *Séférian et al.*, 2014].

The unique ability of diazotrophs to break the strong triple dinitrogen (N_2) bond (enthalpy = +945.5 kJ) makes them a potential long-term winner under climate change-driven reductions in inorganic N fluxes [*Moore and Doney*, 2007]. N_2 fixation by the diverse diazotrophic community has been shown to be a key regulator of the biological carbon pump [*Moisander et al.*, 2010; *Garcia et al.*, 2011]. Estimates show that N_2 fixation rates in the global oceans exceed 180 Tg N yr^{-1} [*Großkopf et al.*, 2012] and that N_2 fixation is able to support up to 50% of the new production in tropical low productivity areas such as the eastern Indian Ocean (IO) [*Raes et al.*, 2014].

Dissolved inorganic nitrogen (DIN) concentrations in the photic zone of the eastern IO are often as low as 0.05 μmol L^{-1} [*Pearce and Pattiaratchi*, 1999], with N:P ratios ~3 such that N strongly limits primary productivity in these oligotrophic waters [*Hanson et al.*, 2007; *Twomey et al.*, 2007]. *Raes et al.* [2014] have shown in this region that the highest DIN concentrations occur at low NO_3^-:NH_4^+ ratios. The latter suggest an active

microbial community controlling mixed layer N and biogenic C fluxes through heterotrophic recycling, as seen in other systems via ammonification [*Bouskill et al*., 2012], nitrification [*Yool et al*., 2007], and N_2 fixation [*Karl et al*., 2002].

In the northern parts of the eastern IO, *Waite et al*. [2013] have highlighted, via compound-specific isotopic measurements of the dissolved NO_3^- pool, that a high fraction of the NO_3^- (40–100%) in the photic zone can be derived from surface N_2 fixation. For most of the oligotrophic waters in this oceanic basin the spatial scales of N_2 fixation and its contribution to the dissolved NO_3^- pool plus the other sources of new and regenerated N remain uncharacterized components of the microbial N cycle.

In this manuscript we elucidate the key regional drivers of primary productivity in the southeastern IO using the physical and biogeochemical data sets from four regional voyages conducted during austral autumn and winter in 2010, 2011, 2012, and 2013. Physical mixing processes, dissolved inorganic nutrients, phytoplankton communities, and nutrient assimilation rates are assessed to investigate N cycling in this region. Our data suggest that part of the new N is delivered to the photic zone via N_2 fixation rather than classic upwelling or mixing processes. We suggest that (a) N_2 fixation products in the photic zone are recycled to NH_4^+ and that (b) these N_2 fixation products are further nitrified (oxidized to NO_2^- and NO_3^-) in relatively lower dissolved oxygen (DO) layers within our study area. We propose that the classic separation between NO_3^- and NH_4^+ as the primary sources of new and recycled N [*Dugdale and Goering*, 1967; *Eppley and Peterson*, 1979] does not hold for these and possibly other similar regions of the world ocean.

2. Material and Methods

2.1. Study Region

We compiled data from four voyages aboard the R/V *Southern Surveyor* (SS) in the southeastern IO between 2010 and 2013 in the region bounded by 28°S–34°S and 110°E and 114°E in middle to late winter of each year (see station locations and time windows, Figure 1). Physical, biogeochemical data and metadata from 169 conductivity-temperature-depth (CTD) stations were accessed through the Integrated Marine Observing System (IMOS, http://www.imos.org.au/). Temperature, salinity, DO, and photosynthetically active radiation (PAR) data were used to describe the physical oceanography, while dissolved inorganic nutrient concentrations including NO_3^-, NO_2^-, NH_4^+, Si, and PO_4^{-3} were used to describe the regional chemical oceanography. Integrated chlorophyll *a* data were also compiled from the four different voyages. Dissolved inorganic nitrogen assimilation data were available from the 2011, 2012, and 2013 voyages. Pigment data and N_2 fixation experiments were conducted during the 2012 and 2013 voyages.

2.2. Biophysical Data

Biophysical parameters were collected using a Seabird SBE911 conductivity-temperature-depth (CTD) profiler mounted on a rosette for all voyages. The profiler was fitted with a Seabird SBE32, 24-Niskin bottle rosette sampler, a Biospherical PAR sensor, a SBE43 O_2 sensor, a Chelsea Aqua tracker Fluorometer, and a Wetlabs C-Star™ transmissometer, with measurements used as a proxy for particle concentration [*Karageorgis et al*., 2008]. Winkler titrations [*Winkler*, 1888] from each individual voyage were used to calibrate the SBE43 O_2 sensor. Linear regression between O_2 sensor and titration data for the respective voyages were $r^2 = 0.9705$ for SS2010v05, $r^2 = 0.9607$ for SS2011v04, $r^2 = 0.9767$ for SS2012v04, and $r^2 = 0.9918$ for SS2013v04. Sea surface heights were derived from satellite altimetry provided via IMOS (http://oceancurrent.imos.org.au/sourcedata/).

2.3. Nutrient Data

Dissolved inorganic nutrients for the SS2010v05 and SS2011v04 voyages were analyzed with a Lachat Autoanalyzer and with a Bran + Luebbe AA3 HR segmented flow analyzer during the SS2012v04 and SS2013v04 voyages. Nutrients were analyzed aboard the ship following standard spectrophotometric methods [*Hansen and Koroleff*, 2009]. NO_3^-/NO_2^- was analyzed according to *Armstrong et al*. [1967] and *Grasshoff et al*. [2009] with detection limits to 0.015 $\mu mol\,L^{-1}$. Phosphate was analyzed according to *Murphy and Riley* [1962] with detection limits to 0.01 $\mu mol\,L^{-1}$. Silicate was determined according to *Grasshoff et al*. [2009] with detection limits to 0.01 $\mu mol\,L^{-1}$. NH_4^+ concentrations were obtained according to *Kérouel and Aminot* [1997], later adapted by *Watson et al*. [2004] with detection limits to 0.004 $\mu mol\,L^{-1}$. All calibration curves

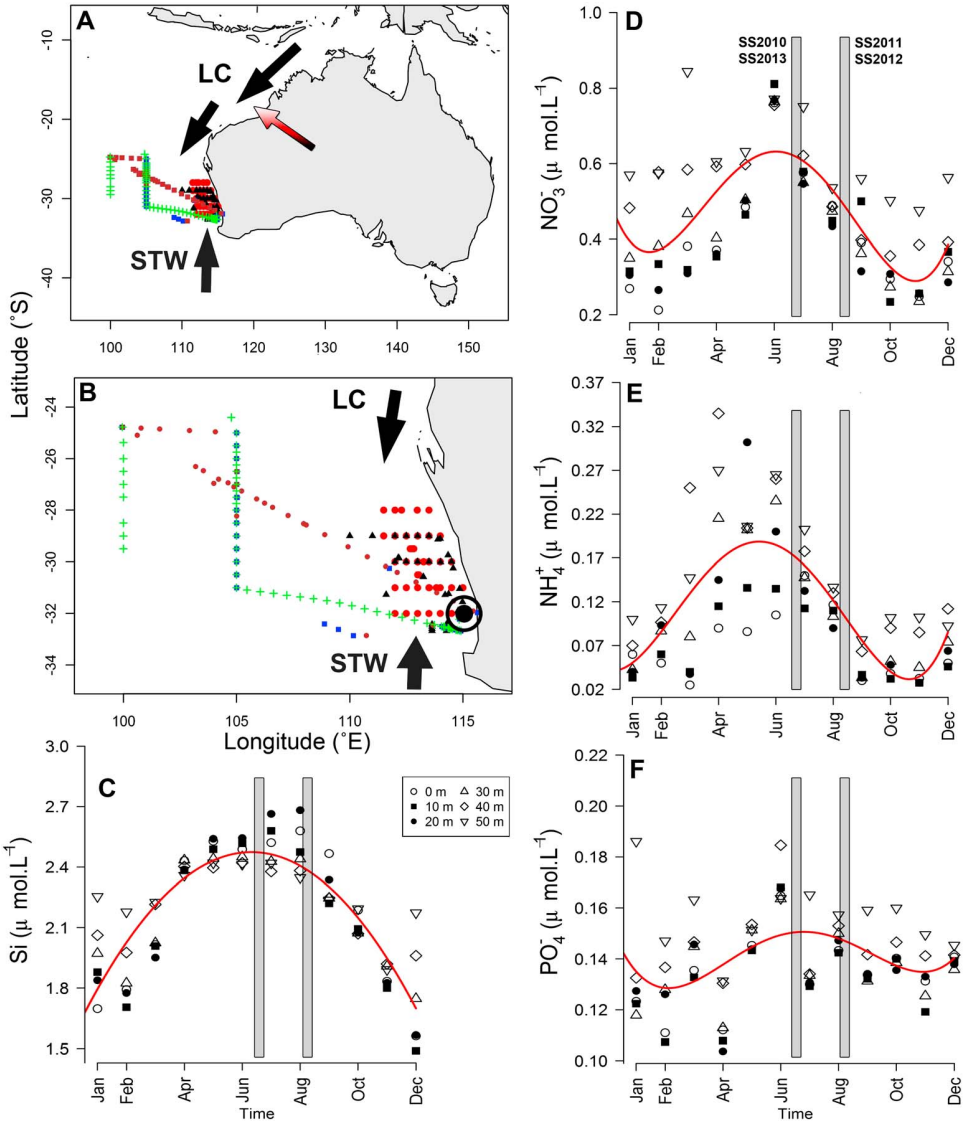

Figure 1. Area map with voyage tracks and CTD stations in detail. (b) Red circles for the SS2010v05 CTD stations; black triangles for SS2011v04 CTD stations; blue squares the CTD stations and brown circles for the flow through stations for the SS2012v04; and green crosses for SS2013v04 voyage CTD stations. Arrows indicate poleward flowing Leeuwin Current (LC) and Northward flowing Subtropical Water (STW). Red gradient arrow indicates major dust inputs according to *McGowan and Clark* [2008]. (c–f) Monthly averaged nutrient concentrations from 1951 to 2014 from the Rottnest National reference station (32.002°S; 114.416°E; Black circle on map in Figure 1b). All concentrations are in μmol L^{-1}. Silicate (Figure 1c) red line second-degree polynomial fit ANOVA $p < 0.0001$, NO_3^- (Figure 1d) red line denotes fourth-degree polynomial fit ANOVA $p < 0.0001$; NH_4^+ concentrations (Figure 1e) were only available from 2010 to 2014, red line denotes fourth-degree polynomial fit ANOVA $p < 0.0001$; and PO_4^- (Figure 1f), red line fourth-degree polynomial fit ANOVA $p < 0.01$. Grey bars indicate when the voyages were conducted.

had an r^2 of 0.999. Coefficients of variation were 0.2% for NO_3^- and NO_2^-, 0.4% for PO_4^{3-}, 0.2% for NH_4^+, and 0.5% for Si. Long-term nutrient data (1951–2014) from the national reference station located near Rottnest Island (32.002°S; 114.416°E) were sourced from the Integrated Marine Observing System (http://imos.org.au).

Voyage-specific high-resolution NO_3^- data were derived from a third polynomial correlation between temperature and in situ NO_3^- bottle data [*King and Devol*, 1979; *Kamykowski et al.*, 2002]. Water mass-specific r^2 for the polynomials for the Leeuwin Current (LC) waters were $r^2 = 0.755$, 0.964, 0.567, and 0.637 in 2010, 2011, 2012, and 2013, respectively. For the Subtropical waters (STWs), we found $r^2 = 0.967$, 0.982, 0.9664,

and 0.815 in 2010, 2011, 2012, and 2013, respectively. Mixed layer depths (MLDs) were calculated according to *de Boyer Montegut et al*. [2004] as a ΔT decrease of 0.4°C compared to a reference value at 6 m depth. As a comparison MLDs were also calculated as the depth where the potential density increased with 0.125 kg m^{-3} to a reference value at 6 m. These MLDs were rejected as they were inconsistent compared to the thermoclines from various CTD casts. We note that for all voyages all CTD casts were deeper than the MLD which is important to note as *Greenwood and Craig* [2014] reported that the MLD often extends to the seabed on the shelf in our study region. Two widely used diffusive coefficients ($Kz_{1\text{-}2}$) (0.1 and 0.37 $cm^2\ s^{-1}$) for oligotrophic waters were used to estimate a first-order range of the injection of new N over the mixed layer depth to provide a broader context of the supply of new N (*Lewis et al*. [1986] and *Oschlies* [2002], respectively). Flux calculations ($FNO_3^- = Kz_{1\text{-}2}\ dNO_3^-/dz$) were performed for the depth interval from 25 m below the MLD to 5 m above the MLD.

2.4. Biological Data

Chlorophyll *a* extractions were carried out according to *Parsons et al*. [1984] on 1 L water samples, using 25 mm Glass Microfiber Filter filters through gentle vacuum filtration (pressure drop < 10 kPa) at six sampling depths (up to100 m). Samples were measured on a Turner design 10 AU fluorometer (for voyages SS2010v05 and SS2011v04) and on a Turner Trilogy fluorometer (for voyages SS2012v05 and SS2013v04). Pigment-specific analysis was carried out on 4 L water samples, using 25 mm Whatman GF/F filters through gentle vacuum filtration (pressure drop < 10 kPa). Pigments were analyzed to determine the phytoplankton communities using high-performance liquid chromatography (HPLC) according to the Commonwealth Scientific and Industrial Research Organisation (CSIRO) methods, see chapter 2 in *Hooker et al*. [2012]. Processed HPLC data were analyzed using the diagnostic pigments of the dominant phytoplankton taxonomic groups and are described in detail by *Vidussi et al*. [2001], *Hirata et al*. [2008], and *Aiken et al*. [2009]. All pigment data were quality controlled according to *Aiken et al*. [2009]. Our data showed that (1) the total Chl *a* (chlorophyll *a*; TChl *a*) made up at least 70% of the total pigment concentration and (2) the regression between TChl *a* and the accessory pigments had a slope of 1.1 and $r^2 > 0.9$. The microplankton community was defined as the sum of the diatom proportion (Fucoxanthin) and the dinoflagellate proportion (Peridinin) over the diagnostic pigments (DPs). The Nanoflagellate community was defined by the Alloxanthin +19′-Butanoyloxyfucoxanthin + Chlorophyll β + 19′-Hexanoyloxyfucoxanthin/DP ratio and the picoplankton community by the Zeaxanthin/DP ratio (see supporting information Table S1 for phytoplankton pigment abbreviations).

2.5. Assimilation Rates

Stable isotope tracers (^{15}N) were used to measure DIN assimilation rates during the 2011, 2012, and 2013 voyages. Dual labeling experiments with $NaH^{13}CO_3$ and ^{15}N tracers were conducted during the 2011 and 2013 voyages. During these voyages 20 μmol L^{-1} of $NaH^{13}CO_3$ was added simultaneously to incubation bottles that were inoculated with ^{15}N tracers including $K^{15}NO_3^-$, $^{15}NH_4Cl$, and $^{15}N_2$ [*Waite et al*., 2007a]. Water samples were taken at the surface (SFC), the deep chlorophyll maximum and at two additional depths for the 2011 voyage and at the surface (SFC; 6 m), and at the depth where O_2 concentrations showed a local depletion (100–150 m) for the 2012 and 2013 voyages. All polycarbonate incubation bottles were acid washed prior to sampling and rinsed 3 times with seawater directly from sample point prior to incubation. Assimilation rate experiments were initiated by adding a known concentration of 0.05 μmol L^{-1} of $K^{15}NO_3$ and $^{15}NH_4Cl$ [*Knap et al*., 1996; *Waite et al*., 2007a]. The inoculated water samples were incubated for 6 h (from 8:00 h −14:00 h) during the 2011 voyage and for 24 h during the 2012 and 2013 voyages. Regardless of incubation time all assimilation rates were in line with earlier recorded measurements [*Hanson et al*., 2007; *Waite et al*., 2007a]. Polycarbonate bottles were placed in on-deck incubators where temperature regulation was maintained by a continuous surface seawater flow. A range of neutral density screens were used to mimic light attenuation at different depths.

Limitations during the study were that NO_3^- and NH_4^+ concentrations were unknown prior to the incubation experiments. We therefore based our spike concentrations on the trace additions of *Waite et al*. [2007a], *Twomey et al*. [2007], and *Hanson et al*. [2007]. Trace additions exceeding 10% did not enhance assimilation rates in our study area ($r^2 = 0.003$, slope = −0.0018, $p = 0.57$, $n = 120$ for NO_3^- assimilation rates and $r^2 = 0.073$, slope = −0.0106, $p = 0.0019$, $n = 129$ for NH_4^+ assimilation rates, respectively; see supporting information Figure S1).

N_2 fixation experiments during the 2012 voyage were conducted simultaneously using the methods described in *Montoya et al*. [1996] and according to *Mohr et al*. [2010], where the direct addition of $^{15}N_2$ tracer-enriched seawater was used as an alternative method to quantify N_2 fixation rates [*White*, 2012]. For the *Montoya et al*. [1996] methodology 5 mL $^{15}N_2$ gas at atmospheric pressure was added to the 4.5 L polycarbonate incubation bottles. For the *Mohr et al*. [2010], degassed and filtered (Sterivex filter 0.2 μm) YBC-II media was spiked with 1 mL $^{15}N_2$ (98 atom%; Aldrich) gas per 100 mL and incubations were initiated by introducing aliquots of $^{15}N_2$ tracer-enriched seawater of 2.6% of the total incubation volume (4.5 L polycarbonate bottle) [see *Raes et al*., 2014]. During all experiments, the incubation bottles were gently rocked ~50 times to enhance mixing prior to 24 h incubation. The solubility of the N_2 concentration in seawater was calculated according to *Hamme and Emerson* [2004]. The recent discovery of potential contamination of $^{15}N_2$ gas with other forms of ^{15}N [*Dabundo et al*. 2014] cannot be ruled out; but if present, these contaminants had a negligible effect as our results clearly show a significant difference between the uptake of N_2, NO_3^-, and NH_4^+ (Figure 5). We also measured different N_2 fixation rates throughout the water column and between stations (contamination would give equal rates throughout the water column). We note that we used the same $^{15}N_2$ batch for a latitudinal transect presented in *Raes et al*. [2014]. Along this latitudinal transect all biotic and abiotic parameters as well as N_2 fixation rates correlated with latitude. Again, contamination would have skewed N_2 fixation rates. Lot number for the used $^{15}N_2$ gas canister was # SZ1670V.

Here we report that the regression slope between the bubble and the dissolution method (slope = 0.51, $r^2 = 0.72$, $n = 30$, and $p < 0.0001$) from our measurements was very similar to the slope reported by *Großkopf et al*. [2012] (slope = 0.59, $r^2 = 0.6$). Our data compliment the discussion that N_2 fixation rates are underestimated when using the bubble method as highlighted by *Mohr et al*. [2010] and *White* [2012]. The N_2 fixation rates that are presented below are only derived from bioassays using the dissolution method.

All assimilation and fixation experiments were terminated by filtering each bottle (pressure drop < 10 kPa) through a 25 mm precombusted GF/F filter. Natural abundance samples of particulate organic carbon/particulate organic nitrogen, used as *t* zero values to calculate assimilation rates, were obtained by filtering 4 L water samples onto precombusted GF/F filters. Filters were snap frozen in liquid N and stored at −80°C. Filters were later acidified and dried overnight at 60°C. Determination of total C, total N, $\delta^{13}C$, and $\delta^{15}N$ were carried out using a continuous flow system consisting of a SERCON 20-22 mass spectrometer connected with an Automated N and C Analyzer. Multipoint normalization was used in order to reduce raw values to the international scale [*Paul et al*., 2007]. Error propagation for stable isotope data was performed as described by *Skrzypek et al*. [2010]. The external error of analyses (1 standard deviation) was 0.15‰ for $\delta^{13}C$ and 0.20‰ for $\delta^{15}N$. Nitrogen assimilation and C fixation rates (ρ in nmol N or C L^{-1} h^{-1}) were calculated following *Dugdale and Goering* [1967] and *Knap et al*. [1996].

2.6. Data Analysis

In situ oxygen, temperature, salinity, fluorescence, and PAR data within the mixed layer for each CTD station were analyzed using principal coordinate analysis (PCA) to separate the physical properties of the different water masses for each voyage. Nutrient concentrations for each CTD station were averaged over the MLD, samples size for averages are given in the text. Trapezoidally depth integrated Chl *a* values were derived from six sampling depths per CTD station down to 100 m for all voyages. Trapezoidally depth integrated NO_3^-, NH_4^-, and C assimilation rates from the SS2011v04 voyage were derived from four sampling depths per CTD station down to 100 m. Statistical analyses including PCAs, two- and one-way analysis of variance (ANOVA) tests were performed using the statistical package R v3.0.1 [*R Development Core Team*, 2013].

3. Results

3.1. Physical Oceanography

We grouped our CTD stations into two water masses based on temperature (*T*), salinity (*S*), dissolved O_2 (DO), fluorescence, and photosynthetic active radiation (PAR). Scatterplots, based on the principal coordinate (PC) loadings, visualized the clustering of the different stations into Subtropical water (STW $n = 79$ CTD stations) and Leeuwin Current water (LC $n = 98$ CTD stations) for all voyages (Figure S2). Temperature, salinity, and dissolved O_2 concentrations explained more than 50% of the variance (first PCs; Figure S2 and Table 1).

Table 1. Yearly Comparison Between the Leeuwin Current and Subtropical Waters of the Physical and Biochemical Parameters From Four Consecutive Voyages in the Eastern IO[a]

	2010		2011		2012		2013		Mean	
To MLD	LC	STW	LC	STW	LC	STW	LC	STW	LC	STW
Temperature (°C)	**21.2 ± 0.5**	18.7 ± 0.5	**20.1 ± 0.5**	17.6 ± 1.0	**20.3 ± 0.7**	18.7 ± 1.0	**21.0 ± 0.7**	19.1 ± 0.8	**20.7 ± 0.76**	18.7 ± 0.9
Salinity (psu)	35.5 ± 0.1	**35.8 ± 0.1**	35.2 ± 0.1	**35.5 ± 0.2**	35.3 ± 0.1	**35.7 ± 0.1**	35.4 ± 0.2	**35.7 ± 0.1**	35.3 ± 0.2	**35.7 ± 0.15**
O_2 (μmol L^{-1})	223 ± 4	**235 ± 3**	231 ± 4	**244 ± 8**	227 ± 5	**236 ± 4**	223 ± 6	**234 ± 5**	227 ± 6	**237 ± 6**
Chl *a* (μgL^{-1})	**0.41 ± 0.19**	0.29 ± 0.14	0.33 ± 0.15	0.25 ± 0.12	**0.43 ± 0.16**	0.24 ± 0.10	0.32 ± 0.14	0.30 ± 0.14	**0.38 ± 0.17**	0.28 ± 0.13
NO_3^- (μmol L^{-1})	**0.30 ± 0.287**	0.1 ± 0.179	0.11 ± 0.192	0.09 ± 0.225	0.07 ± 0.122	0.04 ± 0.136	**0.17 ± 0.334**	0.07 ± 0.190	**0.18 ± 0.276**	0.08 ± 0.188
NO_2^- (μmol L^{-1})	-	-	-	-	0.04 ± 0.037	0.05 ± 0.093	**0.05 ± 0.076**	0.01 ± 0.016	**0.04 ± 0.051**	0.02 ± 0.042
NH_4^+ (μmol L^{-1})	**0.06 ± 0.059**	0.03 ± 0.021	0.03 ± 0.024	0.02 ± 0.018	-	-	0.06 ± 0.049	0.06 ± 0.051	0.05 ± 0.072	0.04 ± 0.038
Si (μmol L^{-1})	**2.7 ± 0.19**	2.2 ± 0.17	**2.3 ± 0.17**	1.9 ± 0.29	**2.7 ± 0.18**	2.3 ± 0.24	**2.7 ± 0.40**	2.2 ± 0.27	**2.6 ± 0.29**	2.2 ± 0.27
PO_4^- (μmol L^{-1})	0.09 ± 0.016	0.09 ± 0.019	0.07 ± 0.018	0.07 ± 0.031	**0.07 ± 0.018**	0.05 ± 0.016	**0.07 ± 0.029**	0.06 ± 0.025	**0.08 ± 0.025**	0.07 ± 0.027

[a]Yearly comparison between LC and STW water masses are in bold ($p < 0.01$); data are average ±standard deviation (SD); $n = 45$ CTD stations for 2010, $n = 38$ CTD stations for 2011, $n = 33$ CTD stations for 2012, and $n = 58$ CTD stations for 2013.

The mean mixed layer depths in the LC (100 ± 54 m ± standard deviation (SD)) and in the STW (92 ± 29 m ±SD) were not significantly different (one-way ANOVA $p = 0.615$). Dissolved O_2 concentrations were always significantly lower in the poleward flowing LC than in the STW (Table 1). Layers of relatively lower dissolved O_2 [*Thompson et al.*, 2011] were observed between 100 and 250 m within and below the mixed layer depth during all voyages (see supporting information Figure S3c) and were associated with warm, low-density, and low-salinity waters. Localized reductions in transparency, an indication of increased particle concentrations, were associated with LC waters (data not shown). Local hot spots of O_2 depletion also occurred within warm core eddies (<180–220 μmol L^{-1}; 100–250 m; see Figure S4).

3.2. Chemical Oceanography

Across the 4 years, mean NO_3^- concentrations within the mixed layer in the LC were 0.2 μmol L^{-1} ($n = 349$) and were significantly higher than average NO_3^- concentrations in the STW (0.08 μmol L^{-1}, $n = 303$; Table 1). Nitrite concentrations were elevated (up to 0.3 μmol L^{-1}) at reduced O_2 concentrations ~180–200 μmol L^{-1} between 100–250 m at the base of the LC. Warmer LC waters had lower O_2 and higher NO_2^- concentrations than the STW (Table 1). The shape of vertical profiles of nutrients, especially in deep mixed layers (MLD ~200 m), will have a significant bearing on the calculation of the vertical NO_3^- flux (see below). The vertical profile of NO_3^- within the LC showed a small but significant increase with increasing MLD, (slope = 0.0016 μmol L^{-1} m^{-1}; Figure S5a). In the STW distribution of NO_3^- was uniform within the mixed layer (Figure S6a).

Average NH_4^+ concentrations were 5 times lower than the average NO_3^- concentrations in the surface mixed layer. NH_4^+ concentrations were significantly greater in the LC than the STW in 2010 only (Table 1). Across all years, NH_4^+ concentrations were marginally higher in the LC waters than the STW (one-way ANOVA $p = 0.06$). The vertical profile of NH_4^+ was uniform in both water masses (Figures S5b and S6b).

The LC carried greater mixed layer PO_4^{-3} concentrations than the STW (Table 1), with a small yet significant increase with depth (slope = 0.002; Figure S5c). In the STW waters PO_4^{-3} concentrations were uniform within the MLD (Figure S6c). NO_3^-:PO_4^{-3} ratios in the LC were higher than in the STW (one-way ANOVA $p < 0.001$; in the LC, NO_3^-:$PO_4^{-3} = 2 \pm 2.2$ (±SD, $n = 347$) versus 1 ± 1.6 (±SD, $n = 296$) in the STW.) These NO_3^-:PO_4^{-3} ratios are ~5 to 10% of global ratios [e.g., *Redfield*, 1958] and highlight the oligotrophic and N-limited nature of this ecosystem.

The eastern Indian Ocean is low in DIN and phosphate but showed high concentrations of silicate (up to 4.7 μmol L^{-1}). The LC plays a role as a silicate source [*Lourey et al.*, 2006]

Table 2. Diffusive NO_3^- Fluxes Over the Mixed Layer Depth in the Leeuwin Current (LC) and Subtropical Waters (STW) in the Eastern IO[a]

	LC		STW	
Voyages	Kz_1(μmol m^{-2} d^{-1})	Kz_2(μmol m^{-2} d^{-1})	Kz_1(μmol m^{-2} d^{-1})	Kz_2(μmol m^{-2} d^{-1})
2010	1.6 ± 2.09	5.5 ± 7.04	9.7 ± 8.53	32.6 ± 28.69
2011	1.9 ± 1.09	6.5 ± 3.68	3.4 ± 5.42	11.3 ± 18.26
2012	1.2 ± 1.87	4.0 ± 6.30	4.4 ± 5.78	14.9 ± 19.46
2013[b]	3.4 ± 1.95	11.5 ± 6.56	6.3 ± 7.42	21.3 ± 24.9

[a]Average ±standard deviation (SD) $n = 45$ CTD stations for 2010; $n = 38$ CTD stations for 2011; $n = 33$ CTD stations for 2012; $n = 58$ CTD stations for 2013. The average gradient over the MLD in the LC was 2.2 ± 2.1 (± SD; $n = 89$) and 6.7 ± 7.87 (± SD; $n = 75$) in the STW.
[b]The NO_3^- flux in 2013 was significantly greater in the LC relative to all other years (one-way ANOVA: for the 2013 and 2012 voyages $p < 0.001$; for 2013 and 2011 voyages $p < 0.05$; and for 2013 and 2010 voyages $p < 0.01$).

as Si concentrations were always higher in the LC waters than the STW (Table 1). Mean ML Si:NO_3^- ratios in the STW (~30) were double those in the LC (~15). The vertical profile of Si in the MLD increased slightly with depth in both water masses (LC slope = 0.0014 μmol L^{-1} m^{-1} and STW slope = 0.0011 μmol L^{-1} m^{-1}; Figures S5d and S6d).

To provide a regional context for a N budget, supporting the DIN assimilation data (see DIN assimilation data below), we estimated a first-order diffusive injection of new N (NO_3^-) over the mixed layer. To calculate this diffusive injection, we used high-resolution NO_3^- data which we derived from temperature and in situ NO_3^- correlations (see section 2). Average NO_3^- concentrations 25 m below the mixed layer depth ranged from 0.3–0.6 μmol L^{-1} in the LC and from 0.07–0.2 μmol L^{-1} in the STW across the 4 years. Although NO_3^- concentrations were overall higher in the LC waters the NO_3^- gradient (from 25 m below the MLD to 5 m above the MLD) in the STW was 3 times greater (steeper slope) compared to the LC waters (Table 2). Two widely used diffusive coefficients (Kz, 0.1 and 0.37 cm^2 s^{-1}) for oligotrophic waters were used to estimate a vertical NO_3^- flux over the mixed layer depth. Average fluxes ranged from 1.6 to 11.5 μmol m^{-2} d^{-1} in the LC and from 3 to 32 μmol m^{-2} d^{-1} in the STW (Table 2). The diffusive injection of new N in the euphotic zone is ~3 times lower in LC waters, highlighting the upwelling suppressing nature of the poleward flowing Leeuwin Current.

3.3. Seasonal Changes

To nest this analysis in a broader temporal picture of the oligotrophic nature of our region, we analyzed nutrient data over a 60 year period. The data, collected from five depths (0–50 m) from the national reference station at Rottnest Island in the southern quadrant of our research area, highlight the seasonal trend of nutrient concentrations in the eastern IO (Figures 1c–1f). We note that despite significant seasonal fluctuations, the average DIN and PO_4^- concentrations always remained < 1 μmol L^{-1}. NO_3^- concentrations showed a significant increase (up to 0.8 μmol L^{-1}) in June, whereas NH_4^+ concentrations displayed a peak between April and June around 0.3 μmol L^{-1}. Phosphate showed the lowest degree of temporal variability, with concentrations showing a minimal increase around June. Of all nutrients, silicate concentrations had the clearest temporal variability, increasing from April through September (Figures 1c–1f).

3.4. Biological Oceanography

3.4.1. Pigments

The oligotrophic nature of the eastern Indian Ocean relates to an overall low (~0.35 μg L^{-1}) standing phytoplankton stock (Table 1). Although the average Chl *a* concentrations were significantly greater in the LC than in the STW during the 2010 and 2012 voyages (Table 1), no significant differences were found for the depth-integrated Chl *a* concentrations between the two water masses across all other years (one-way ANOVA $p > 0.2$ for all voyages). We therefore combined the LC and STW stations to get a regional picture of Chl *a* concentrations in the eastern IO. Depth-integrated Chl *a* concentrations from four austral voyages averaged 42 ± 15 mg m^{-2} and showed a positive correlation with sea surface height across all years (Figure 2).

3.4.2. Communities

Regionally, the nanoplankton represented the bulk (~60%) of the functional phytoplankton communities. Nanoplankton was the most abundant with a mean fraction of 0.59 ± 0.17, where after pico plankton with

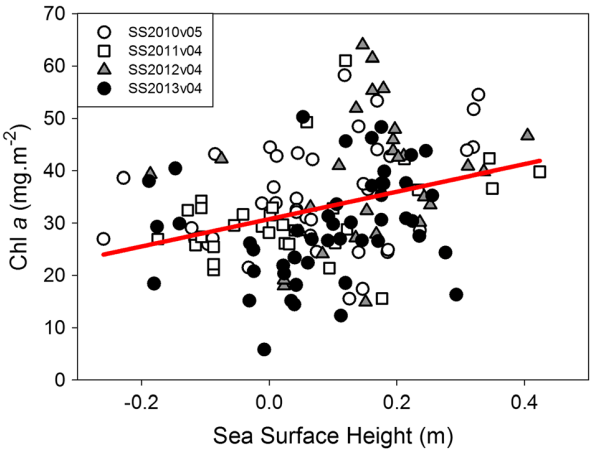

Figure 2. Depth-integrated Chl *a* concentrations (mg m^{-2}) plotted against sea surface height (m). Red line presents linear regression $r^2 = 0.11$, $p < 0.0001$, slope = 38, $n = 149$.

a mean of 0.33 ± 0.18, followed by the microplankton fraction with a mean of 0.08 ± 0.04 (±SDs; Figure 3). The phytoplankton size fractions were all significantly different from each other (Dunn's multiple comparison test $p < 0.005$) and did not vary interannually (Figure 3).

3.4.3. NH_4^+ and NO_3^- Assimilation Rates

NH_4^+ and NO_3^- assimilation rates were not significantly different between the two water masses in 2011 or 2012, and rates from the two water masses were therefore pooled to get a regional picture of DIN incorporation rates. Regional depth-integrated NH_4^+ assimilation rates in 2011 (532 ± 217 μmol m^{-2} h^{-1}) were significantly higher than NO_3^- assimilation rates (327 ± 217 μmol m^{-2} h^{-1}; one-way ANOVA $p < 0.001$; Table 3). In 2012 regional NH_4^+ assimilation rates were not significantly different than NO_3^- assimilation rates, despite higher maxima (one-way ANOVA $p = 0.155$; Table 3). In 2013, NH_4^+ assimilation rates were higher than NO_3^- assimilation rates in LC waters than in STW (one-way ANOVA $p < 0.01$). No significant differences, however, were found for the NO_3^- assimilation rates in the LC and STW (one-way ANOVA $p = 0.345$).

From a regional perspective NH_4^+ assimilation rates were 68% greater relative to the NO_3^- assimilation rates (one-way ANOVA $p < 0.001$; Table 3). Across three cruises in 2011, 2012, and 2013 the maximum assimilation of NH_4^+ was consistently greater, and in some years up to 2.7 times greater, compared to the NO_3^- assimilation rates (Table 3), there was no significant difference between the NH_4^+ assimilation means across the years (one-way ANOVA $p = 0.155$).

3.4.4. N_2 and C Fixation

Regionally, during the 2012 voyage, N_2 fixation rates ranged from 0.1 to 12.6 nmol L^{-1} h^{-1} (Table 3). N_2 fixation rates were much lower in the relatively lower oxygenated layers (~180 μmol L^{-1}) compared to well-oxygenated surface waters (Figure 4). During our 2013 voyage regional N_2 fixation rates were significantly smaller from those found in the previous year (one-way ANOVA $p < 0.01$ Table 3). In both years N_2 fixation rates in the LC were significantly greater compared to the rates in the STW (one-way ANOVA's $p < 0.01$; Figure 4). We did not depth integrate our N_2 fixation rates as we only had two vertical measurements; one at the surface (6 m) and one in the lower oxygenated waters (~100–200 m).

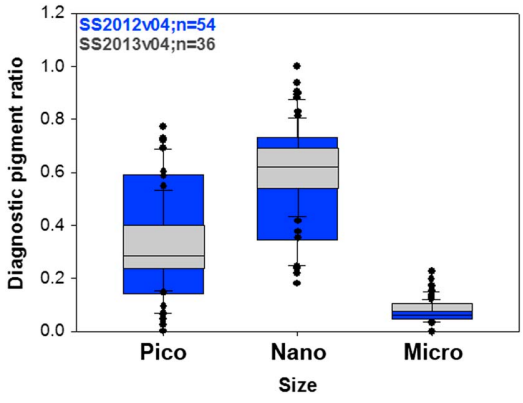

Figure 3. Phytoplankton community composition in the eastern IO. Size classes picophytoplankton (Pico), nanophytoplankton (Nano) and microphytoplankton (Micro) for the SS2012v04 and SS2013v04 voyages. Interannually, the phytoplankton community composition did not show a significant difference in their size structures in the LC or the STW. One-way ANOVA, $p = 0.843$, $p = 0.584$, and $p = 0.562$ for the micro, nano, and pico size classes in the LC, respectively; and one-way ANOVA, $p = 0.078$, $p = 0.812$, and $p = 0.969$ for the micro, nano, and pico size classes in the STW, respectively.

Carbon fixation rates averaged 21.7 ± 6.11 nmol L^{-1} h^{-1} (SD, $n = 102$) in 2011 and 21.3 ± 16.16 nmol L^{-1} h^{-1} (SD, $n = 32$) in 2012, and were not significantly different between the LC and the STW (one-way ANOVA $p = 0.254$). Dual labeling experiments (^{15}N and ^{13}C), during the 2013 voyage, showed that all DIN assimilation rates correlated positively with C fixation rates

Table 3. Regional Dissolved Inorganic Nitrogen Assimilation Rates in the Eastern IO

Voyage		NH_4^+ Assimilation (nmol L^{-1} h^{-1})	NO_3^- Assimilation (nmol L^{-1} h^{-1})	N_2 Fixation (nmol L^{-1} h^{-1})
SS2011vo4	min	0.03	0.01	-
	max	19.08	14.78	
	aver	5.6 ± 3.95[a] (n = 102)	3.5 ± 3.39 (n = 102)	-
SS2012vo4	min	0.4	0.8	0.1
	max	21.9	8.19	12.6
	aver	9.3 ± 9.14 (n = 12)	3.5 ± 2.15 (n = 21)	4.5 ± 3.8[b] (n = 30)
SS2013vo4	min	0.4	0.03	0.1
	max	14.5	7.83	2.19
	aver	4.8 ± 3.86[a] (n = 34)	1.8 ± 1.76 (n = 38)	0.6 ± 0.50 (n = 39)

[a]One-way ANOVA $p < 0.001$ between NH_4^+ and NO_3^- assimilation during SS2011v04 and SS2013v04.
[b]One-way ANOVA $p < 0.001$ between the N_2 fixation rates measured during the SS2012v04 and SS2013v04 voyages.

(Figure 5). The slope of the DIN assimilation and C fixation rates converted to an apparent C:N ratio of 6 for NH_4^+ assimilation, an apparent C:N ratio of 11.7 for NO_3^- assimilation, and an apparent C:N ratio of 47.8 for N_2 assimilation (Figure 5). However, basing the C:N ratios on single DIN assimilation rates (e.g., C versus NH_4^+ only) could overestimate the true C:N assimilation ratio. The combined ^{13}C: ($^{15}NO_3^- + {}^{15}NH_4^+ + {}^{15}N_2$) ratio, regionally, averaged 4 ± 2.2 (±SD, n = 32).

4. Discussion

4.1. N Cycling in the Indian Ocean

In our study, the water mass separation between the Leeuwin Current (LC) and Subtropical Water Mass (STW) did not necessarily translate into significantly different biological responses such as phytoplankton size classes, biomass, and C and N assimilation rates. We therefore constructed a more regional oceanographic picture of how the N cycle influences primary productivity, nesting this in long-term nutrient data from the Rottnest Island (IMOS http://www.imos.org.au/). We then calculated the diapycnal NO_3^- fluxes and the DIN assimilation rates over the 4 year period of our study, to estimate the overall contribution of N_2 fixation to new N.

The Indian Ocean (IO) is potentially one of the most N-limited regions in the world ocean [*Polovina et al.*, 2008]. The average seasonal distribution of DIN stays below 1 μmol L^{-1}, and N:P ratios average around 12–13 in our study, which are similar to those documented in the World Ocean Circulation Experiment (WOCE) Atlas for the IO [*Talley*, 2013]. Nutrient ratios presented herein from the mixed layer were even lower than the WOCE values, suggesting a preferential net drawdown of N with respect to P. The N-limited nature of this ecosystem is also highlighted in the seasonal data by the excess of PO_4^{-3} and the overabundance of Si in comparison to DIN. The lack of a clear linear relationship between P and N in the mixed layer, and the high level of scatter in our seasonal DIN data at low concentrations, made it difficult to resolve the regional impact of N_2 either from actual nutrient concentrations or from stoichiometric concepts such N* and P* alone [see *Deutsch et al.*, 2001]. Our efforts to calculate a regional N* value did not give any insights despite the fact that N approached the detection limit which suggests the potential for significant N injections through N_2 fixation

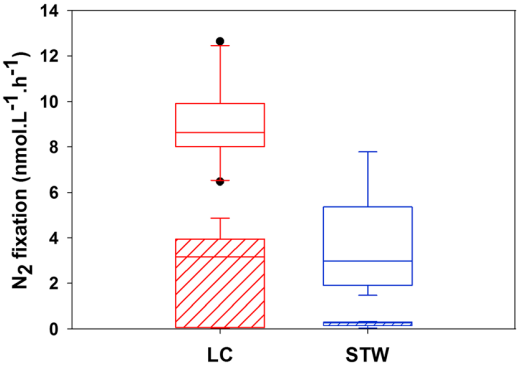

Figure 4. N_2 fixation in Leeuwin Current and Subtropical waters. Nonshaded box presents data from 6 m depth. Shaded boxplot present data from relatively lower dissolved oxygen layers (100–200 m; 100–180 μmol L^{-1}). N_2 fixation rates at 6 m depth were greater in the warmer LC waters compared to the colder STW (one-way ANOVA $p < 0.001$).

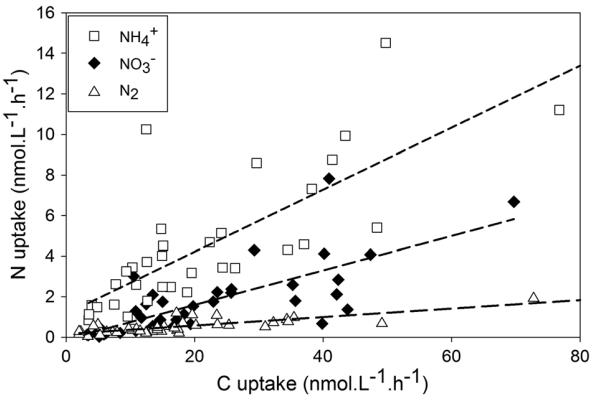

Figure 5. Dissolved inorganic nitrogen assimilation rates (nmol L^{-1} h^{-1}) versus inorganic C fixation rates (nmol L^{-1} h^{-1}) for different N sources. Linear regressions between DIN assimilation rates and C fixation rates were $r^2 = 0.67$, slope = 0.153, $p < 0.0001$, $n = 34$ for NH_4^+ (squares); $r^2 = 0.67$, slope = 0.085, $p < 0.0001$, $n = 38$ for NO_3^- (black diamonds); and $r^2 = 0.71$, slope = 0.021, $p < 0.0001$, $n = 39$ for N_2 (triangles).

[*Weber and Deutsch*, 2014]. The unsuccessful N* calculations highlighted the need for direct flux measurements to resolve the net impact of N_2 fixation, since N pools were low and variable (coefficient of variation of 100%) in comparison to P and Si pools (coefficient of variation of 10%). Understanding the sources of N is therefore important to understand regional primary productivity.

4.2. Regenerated N

In our study the overall 68% higher NH_4^+ assimilation rates relative to NO_3^- assimilation rates suggest that the fixation dynamics of dissolved inorganic carbon are regulated primarily by microbial regeneration of particulate organic matter and dissolved organic matter (DOM) [*Azam et al*., 1994; *Azam*, 1998; *Verdugo et al*., 2004].

Oligotrophic pelagic regions are mostly characterized by the microbial food web where protozoans graze on the picophytoplankton and nanophytoplankton [*Cushing*, 1989]. Low nutrient concentrations favor smaller phytoplankton size classes with a higher affinity for regenerated N [*Dortch*, 1990; *Eppley et al*., 1969]. This correlation is confirmed by our HPLC data as the nanoplankton represented >60% of the phytoplankton community. The higher nutrient affinity of the smaller size fractions in these nutrient-depleted waters, nearly all year round provides a potential explanation for the (relative) paucity of diatoms despite seasonal oversupply of Si.

4.3. New N From Below the MLD

The relatively low volumetric and depth-integrated NO_3^- assimilation rates (<15 nmol L^{-1} h^{-1}; ~375 μmol m^{-2} h^{-1}) were in line with earlier measurements in this region [*Hanson et al*., 2007; *Waite et al*., 2007a]. The estimated vertical diffusive NO_3^- fluxes, however, over the mixed layer depth were 10 times lower than the reported fluxes from the open Atlantic ~140 μmol m^{-2} d^{-1} [*Lewis et al*., 1986], but of similar order to the fluxes reported by *Planas et al*. [1999] in the North Atlantic subtropical gyre ~50 μmol m^{-2} d^{-1}. Depth-integrated NO_3^- assimilation rates thus exceeded the diffusive flux (~1–30 μmol m^{-2} d^{-1}; Table 2) by a factor of 100. *Planas et al*. [1999] noted a strong nonlinear relationship between NO_3^- assimilation rates and the deep NO_3^- supply. They reported that NO_3^- assimilation rates exceeded the deep NO_3^- flux by a factor of 5 in the oligotrophic central Atlantic. Elevated assimilation rates along with the presence of low NO_3^- concentrations are typical in recently upwelled waters nearing the end response of a phytoplankton bloom [*Dugdale et al*., 1990]. The latter scenario is, however, not relevant to the southeastern IO as the poleward flowing LC suppresses upwelling [*Waite et al*., 2007b] and NO_3^- concentrations are always relatively low (see seasonal data). Although NO_3^- assimilation was consistently a small fraction of the total N assimilation, it is clear that a simple vertical diffusive flux still does not suffice to supply the measured NO_3^- demand. Therefore, an alternative NO_3^- source must be identified to complete the N mass balance for the region.

4.4. Other Potential N Sources

Warm core eddies (positive sea surface heights) are a common feature of the Leeuwin Current [*Feng et al*., 2007] and have been shown to exhibit locally enhanced primary productivity via a variety of mechanisms, including cross-shelf nutrient enrichment [*Waite et al*., 2015], frictional decay [*Franks et al*., 1986], retention of nutrients [*Greenwood et al*., 2007], injection of new N through N_2 fixation [*Fong et al*., 2008], seasonal deepening of the mixed layer due to heat loss and pycnocline deflection [*Pearce and Feng*, 2007]. Other sources of NO_3^- could be the vertical advection of nutrients via submesoscale upwelling which has been documented by *Paterson et al*. [2008] in our study area. We note that on a seasonal scale (especially in winter), the importance of mixed layer nutrient entrainment with a deepening of the MLD, as highlighted by *Dufois et al*. [2014], will be an

important residual source of NO_3^-. The importance of N injections through these events is highlighted by the significantly higher integrated Chl *a* concentrations associated with positive sea surface heights across the study region as seen by *Feng et al.* [2003] and *Waite et al.* [2007b]. These Chl *a* anomalies with positive sea surface heights have been observed to extend beyond the LC region across the whole southern IO [*Brewin et al.*, 2012; *Dufois et al.*, 2014].

Global modeling studies have also highlighted the role of subscale and mesoscale turbulence in providing additional N sources in the euphotic zone [*McGillicuddy and Robinson*, 1998]. Horizontal nutrient transport and nutrient streams [*Williams et al.*, 2006] can enhance new production [*Williams and Follows*, 1998] including the lateral transport of dissolved organic nitrogen (DON) [*Torres-Valdés et al.*, 2009]. When such episodic nutrient injections occur, the contribution of N_2 fixation will have a lower importance. *Oschlies and Garçon* [1998] note that mesoscale turbulence can account for up to one third of the total NO_3^- flux in the subtropics and midlatitudes of the North Atlantic Ocean. Yet they also state that this injection is not sufficient to maintain the observed primary production. Export production, by definition, requires a supply of new nutrients to the euphotic zone to offset sedimentary losses. Again, for the eastern Indian Ocean, sources of N other than cross-pycnocline transport must be considered.

4.5. N_2 Fixation

Besides the possible additional nutrient injections through the mesoscale processes (horizontal and lateral), we measured N_2 fixation rates at all stations during two consecutive years. Our N_2 fixation rates ($<12\,nmol\,L^{-1}\,h^{-1}$) fall between those presented by *Montoya et al.* [2004] in the Timor Sea (20–60 $nmol\,L^{-1}\,h^{-1}$) and those reported by *Großkopf et al.* [2012] in the South Atlantic Ocean (~0.5 $nmol\,L^{-1}\,h^{-1}$). One possible explanation for the relative high rates in the eastern IO compared to the South Atlantic Ocean could be the impact of dust transport, originating from Lake Eyre and from local sources such as the iron-rich Pilbara region [*Morris and Ramanaidou*, 2007]. *McGowan and Clark* [2008] mapped a dust trajectory path that extends over a vast region covering the entire north Australian coast from the Torres Strait (142°E, 10.5°S) to the Northwest Cape (114.5°E, 21°S). The core of the pathway passes over the Great Sandy Desert and the southern Kimberly into the IO and Timor Sea [*McGowan and Clark*, 2008]. Dust deposition into nutrient-poor waters has been shown to stimulate marine productivity [*Boyd et al.*, 2000; *Jickells et al.*, 2005] and N_2 fixation rates [*Mahaffey et al.*, 2004; *Rubin et al.*, 2011].

Our N_2 fixation rates confirm model estimates [*Monteiro et al.*, 2010; *Monteiro et al.*, 2011] demonstrating that these rates in the southeastern IO are globally significant. The model from *Monteiro et al.* [2010] predicts a dominance of unicellular cyanobacterial N_2 fixation in the IO. These model data also support earlier findings from *McInnes et al.* [2014] and *Raes et al.* [2014] where high bulk N_2 fixation rates (~6 $nmol\,L^{-1}\,h^{-1}$) at higher latitudes (~35°S) were attributed to unicellular N_2 fixation. The N_2 fixation rates we have presented here further support the conclusion of *Goebel et al.* [2010] and *Moisander et al.* [2010] that in the eastern Indian Ocean, at least on a local-scale, unicellular N_2-fixing cyanobacteria can have equal or greater N_2 fixation rates than the cyanobacteria *Trichodesmium*.

Although the assimilation of N_2 is highly energetically demanding (enthalpy = +945.5 kJ), suggesting that fixation rates should decline when less expensive N sources are available [*Weber and Deutsch*, 2014], the fixation of N_2 did not decline when other sources of DIN were available in our study region. Our data showed that the diazotrophic community still fixed ~2 $nmol\,L^{-1}\,h^{-1}$ even at relatively elevated NH_4^+ and NO_3^- assimilation rates (~12 $nmol\,L^{-1}\,h^{-1}$ and ~6 $nmol\,L^{-1}\,h^{-1}$, respectively). These data suggest a continuous input of new N through N_2 fixation. With a first-order budget calculation we give a first estimate of how much N_2 fixation contributes toward N assimilation. N_2 fixation rates averaged 2.5 $nmol\,L^{-1}\,h^{-1}$. NH_4^+ assimilation rates averaged 7 $nmol\,L^{-1}\,h^{-1}$ and NO_3^- assimilation rates averaged 2.6 $nmol\,L^{-1}\,h^{-1}$ (see Table 3; 2012 and 2013 voyages). The total DIN assimilation rates averaged 12.1 $nmol\,N\,L^{-1}\,h^{-1}$. The contribution of N_2 toward the total DIN assimilation pool averaged therefore 20% during the winter months in the eastern Indian Ocean, making fixation equal to NO_3^- in terms of N assimilation. Our seasonal nutrient analysis shows that nutrients are elevated during winter months, leaving a potential for still higher N_2 fixation rates during summer. The sequestration of C by the diazotrophic community has been recognized as a core component in oceanic and atmospheric CO_2 coupling [*Falkowski*, 1997; *Douglas*, 2001], yet to date the quantification of N_2 fixation and the associated C sequestration still remains largely unknown, particularly in the IO.

4.6. Further Hypothesis

The entrainment of thin (10–20 m) and shallow (100–200 m) reduced oxygen layers at the base of the Leeuwin Current were detected by *Rochford* [1969] and described by *Woo and Pattiaratchi* [2008]. Their association with biogeochemical anomalies including increased NO_3^- concentrations [*Thompson et al*., 2011] and lowered pH [*Waite et al*., 2013] were identified later. Prior work in the northeastern IO links the oxidation of particulate organic matter associated with Low Dissolved Oxygen High Nitrate layers to the shallow regeneration of NO_3^- sourced from newly fixed N within surface waters (NO_3^- with a $\delta^{15}N$ signature ~0‰) [*Waite et al*., 2013]. From this and our current analysis we hypothesize that NO_3^- can be sourced from the oxidation of the products of N_2 fixation, including particulate organic matter and NH_{4+} in our study area. These concepts compliment the work of *Ward et al*. [1989] where rapid N recycling within the nitracline is highlighted along with the work of *Mahaffey et al*. [2004] where diazotrophs increased the DON pool in the northern oligotrophic subtropical gyre of the Atlantic Ocean. *Mourino-Carballido et al*. [2011] have furthermore shown that N_2 fixation can explain $>$ 40% of the new N entering the euphotic zone in areas with low diffusive NO_3^- fluxes and contribute up to half of the new production [*Karl et al*., 1997]. A NO_3^- excess has further been linked to N_2 fixation in the North Atlantic Ocean by *Hansell et al*. [2004], where they modeled that the injection of NO_3^- through nitrification of N-rich organic matter (derived from N_2 fixation) can be up to 13.5%. *Painter et al*. [2013] showed that the input of new N from N_2 fixation can be equivalent to up to 60% of the diffusive NO_3^- supply and that N_2 fixation could exceed the diffusive flux at certain stations in the eastern subtropical North Atlantic Ocean. Taking these arguments into account, we suggest that the direct and potentially the indirect contributions of N_2 fixation could be an important source of new N in the eastern Indian Ocean. We therefore hypothesize that shallow nitrification could be a likely source for the relative high NO_3^- assimilation rates we observed.

4.7. Conclusion

In this study we have provided evidence that N_2 fixation could be an important source of new N in the eastern Indian Ocean, supporting primary productivity. Although we lack nitrification rate measurements, our results are consistent with the theory of *Thompson et al*. [2011] which suggest that shallow nitrification is a significant component of the N cycle in the eastern IO. Our data complements the results of previous work of *Waite et al*. [2013] and *Raes et al*. [2014] and has advanced our understanding of new N recycling above the pycnocline in the southeastern Indian Ocean. The significance of nitrification above the pycnocline has been highlighted by other authors [*Hansell et al*., 2004; *Yool et al*., 2007; *Ward et al*., 2013; *Ryabenko et al*. 2012], yet global data on nitrification rates in surface waters are sparse. One consequence of surface nitrification is an overestimation of the new N attributed to NO_3^- fluxes [*Yool et al*., 2007]. We therefore hypothesize that as the vertical flux of NO_3^- from below the nutricline is not a dominant source of N that the bulk of the NO_3^- could be derived from new N through N_2-fixation. Thus, new N injected through N_2 fixation could potentially be recycled within the photic zone to NH_4^+ and sequentially oxidized to NO_2^- and NO_3^-. These amonified and oxidized forms of N, derived from N_2 fixation, could thereby potentially act as a new source of bioavailable N in the southeastern Indian Ocean.

Acknowledgments
We thank the captain and Marine National Facility crew of the Southern Surveyor for their technical assistance while at sea. Supporting grants for the SS2010v05 and SS2011v04 came from A.M. Waite. This research was made feasible because Helen Phillips gave us the opportunity to piggyback onto the SS2012v04 and 2013v04 voyages. Eric J. Raes has been supported through an Australian Postgraduate scholarship from the University of Western Australia and a CSIRO Wealth from Oceans postgraduate top-up scholarship. We would like to thank Hannipoula Olsen for the experimental setup at sea. Physical, biogeochemical data and metadata to support this article can be accessed through the Integrated Marine Observing System (IMOS http://www.imos.org.au/). Biological assimilation data sets can be requested through the corresponding author. We sincerely thank the constructive feedback and insightful comments from the anonymous reviewers.

References

Aiken, J., Y. Pradhan, R. Barlow, S. Lavender, A. Poulton, P. Holligan, and N. Hardman-Mountford (2009), Phytoplankton pigments and functional types in the Atlantic Ocean: A decadal assessment, 1995–2005, *Deep Sea Res., Part II Topical Stud. Oceanogr.*, *56*(15), 899–917.
Alexander, D., et al. (2012), *Indian Ocean: A Sea of Uncertainty*, Future Directions Intl., Perth, Australia.
Armstrong, F., C. R. Stearns, and J. D. H. Strickland (1967), The measurement of upwelling and subsequent biological process by means of the Technicon Autoanalyzer® and associated equipment, *Deep Sea Res., Oceanogr. Abstr.*, *14*(3), 381–389.
Azam, F. (1998), Microbial control of oceanic carbon flux: The plot thickens, *Science*, *280*, 694–695.
Azam, F., D. Smith, G. Steward, and Å. Hagström (1994), Bacteria-organic matter coupling and its significance for oceanic carbon cycling, *Microb. Ecol.*, *28*, 167–179.
Bouskill, N. J., D. Eveillard, D. Chien, A. Jayakumar, and B. B. Ward (2012), Environmental factors determining ammonia-oxidizing organism distribution and diversity in marine environments, *Environ. Microbiol.*, *14*(3), 714–729.
Boyce, D. G., M. R. Lewis, and B. Worm (2010), Global phytoplankton decline over the past century, *Nature*, *466*(7306), 591–596.
Boyd, P. W., A. J. Watson, C. S. Law, E. R. Abraham, T. Trull, R. Murdoch, D. C. E. Bakker, A. R. Bowie, K. Buesseler, and H. Chang (2000), A mesoscale phytoplankton bloom in the polar Southern Ocean stimulated by iron fertilization, *Nature*, *407*(6805), 695–702.
Brewin, R. J., T. Hirata, N. J. Hardman-Mountford, S. J. Lavender, S. Sathyendranath, and R. Barlow (2012), The influence of the Indian Ocean Dipole on interannual variations in phytoplankton size structure as revealed by Earth Observation, *Deep Sea Res., Part II: Topical Stud. Oceanogr.*, *77*, 117–127.

Cushing, D. H. (1989), A difference in structure between ecosystems in strongly stratified waters and in those that are only weakly stratified, *J. Plankton Res.*, *11*(1), 1–13.
Dabundo, R., et al. (2014), The contamination of commercial $^{15}N_2$ gas stocks with ^{15}N-labeled nitrate and ammonium and consequences for nitrogen fixation measurements, *PloS One*, *9*(10), e110335, doi:10.1371/journal.pone.0110335.
de Boyer Montegut, C., G. Madec, A. S. Fischer, A. Lazar, and D. Iudicone (2004), Mixed layer depth over the global ocean: An examination of profile data and a profile-based climatology, *J. Geophys. Res.*, *109*, C12003, doi:10.1029/2004JC002378.
Deutsch, C., N. Gruber, R. M. Key, J. L. Sarmiento, and A. Ganachaud (2001), Denitrification and N_2 fixation in the Pacific Ocean, *Global Biogeochem. Cycles*, *15*(2), 483–506, doi:10.1029/2000GB001291.
Dortch, Q. (1990), The interaction between ammonium and nitrate assimilation in phytoplankton, *Mar. Ecol. Prog. Ser.*, *61*(1), 183–201.
Douglas, C. (2001), Marine nitrogen fixation: What's the fuss?, *Curr. Opin. Microbiol.*, *4*(3), 341–348.
Dufois, F., N. J. Hardman-Mountford, J. Greenwood, A. J. Richardson, M. Feng, S. Herbette, and R. Matear (2014), Impact of eddies on surface chlorophyll in the South Indian Ocean, *J. Geophys. Res. Oceans*, *119*, 8061–8077, doi:10.1002/2014JC010164.
Dugdale, R. C., and J. J. Goering (1967), Assimilation of new and regenerated forms of nitrogen in primary productivity, *Limnol. Oceanogr.*, *12*(2), 196–206.
Dugdale, R. C., E. P. Wilkerson, and A. Morel (1990), Realization of new production in coastal upwelling areas: A means to compare relative performance, *Limnol. Oceanogr.*, *35*(4), 822–829.
Eppley, R. W., and B. J. Peterson (1979), Particulate organic matter flux and planktonic new production in the deep ocean, *Nature*, *282*, 677–680.
Eppley, R. W., J. N. Rogers, and J. J. McCarthy (1969), Half-saturation constants for assimilation of nitrate and ammonium by marine phytoplankton, *Limnol. Oceanogr.*, *14*(6), 912–920.
Falkowski, P. G. (1997), Evolution of the nitrogen cycle and its influence on the biological sequestration of CO_2 in the ocean, *Nature*, *387*(6630), 272–275.
Feng, M., G. Meyers, A. Pearce, and S. Wijffels (2003), Annual and interannual variations of the Leeuwin Current at 32°S, *J. Geophys. Res.*, *108*(C11), 3355, doi: 10.1029/2002JC001763.
Feng, M., L. J. Majewski, C. Fandry, and A. M. Waite (2007), Characteristics of two counter-rotating eddies in the Leeuwin Current system off the Western Australian coast, *Deep Sea Res. Part II: Topical Stud. Oceanogr.*, *54*, 961–980.
Fong, A. A., D. M. Karl, R. Lukas, R. M. Letelier, J. P. Zehr, and M. J. Church (2008), Nitrogen fixation in an anticyclonic eddy in the oligotrophic North Pacific Ocean, *ISME J.*, *2*, 663–676.
Franks, P. J., J. Wroblewski, and G. R. Flierl (1986), Prediction of phytoplankton growth in response to the frictional decay of a warm-core ring, *J. Geophys. Res.*, *91*(C6), 7603–7610, doi:10.1029/JC091iC06p07603.
Garcia, N. S., F. X. Fu, C. L. Breene, P. W. Bernhardt, M. R. Mulholland, J. A. Sohm, and D. A. Hutchins (2011), Interactive effects of irradiance and CO_2 on CO_2 fixation and N_2 fixation in the diazotroph *Trichidesmium erythraeum* (Cyanobacteria), *J. Phycol.*, *47*(6), 1292–1303.
Goebel, N. L., K. A. Turk, K. M. Achilles, R. Paerl, I. Hewson, A. E. Morrison, J. P. Montoya, C. A. Edwards, and J. P. Zehr (2010), Abundance and distribution of major groups of diazotrophic cyanobacteria and their potential contribution to N_2 fixation in the tropical Atlantic Ocean, *Environ. Microbiol.*, *12*(12), 3272–3289.
Grasshoff, K., K. Kremling, and M. Ehrhardt (Eds.) (2009), *Methods of Seawater Analysis*, 3rd ed., John Wiley, Weinheim, Germany.
Greenwood, J., and P. Craig (2014), A simple numerical model for predicting vertical distribution of phytoplankton on the continental shelf, *Ecol. Modell.*, *273*, 165–172.
Greenwood, J., M. Feng, and A. Waite (2007), A one-dimensional simulation of biological production in two contrasting mesoscale eddies in the south eastern Indian Ocean, *Deep Sea Res., Part II Topical Stud. Oceanogr.*, *54*(8), 1029–1044.
Großkopf, T., W. Mohr, T. Baustian, H. Schunck, D. Gill, M. M. Kuypers, G. Lavik, R. A. Schmitz, D. W. Wallace, and J. LaRoche (2012), Doubling of marine dinitrogen-fixation rates based on direct measurements, *Nature*, *488*(7411), 361–364.
Hamme, R. C., and S. R. Emerson (2004), The solubility of neon, nitrogen and argon in distilled water and seawater, *Deep Sea Res., Part I*, *51*(11), 1517–1528.
Hansell, D. A., N. R. Bates, and D. B. Olson (2004), Excess nitrate and nitrogen fixation in the North Atlantic Ocean, *Mar. Chem.*, *84*(3), 243–265.
Hansen, H. P., and F. Koroleff (2009), Determination of nutrients, in *Methods of Seawater Analysis*, edited by K. Grasshoff, K. Kremling, and M. Ehrhardt, pp. 159–228, John Wiley, Weinheim, Germany.
Hanson, C. E., A. M. Waite, P. A. Thompson, and C. B. Pattiaratchi (2007), Phytoplankton community structure and nitrogen nutrition in Leeuwin Current and coastal waters off the Gascoyne region of Western Australia, *Deep Sea Res., Part II Topical Stud. Oceanogr.*, *54*(8–10), 902–924.
Hirata, T., J. Aiken, N. Hardman-Mountford, T. Smyth, and R. Barlow (2008), An absorption model to determine phytoplankton size classes from satellite ocean colour, *Remote Sens. Environ.*, *112*(6), 3153–3159.
Hollowed, A. B., M. Barange, R. J. Beamish, K. Brander, K. Cochrane, K. Drinkwater, M. G. Foreman, J. A. Hare, J. Holt, and S.-I. Ito (2013), Projected impacts of climate change on marine fish and fisheries, *ICES J. Mar. Sci.*, *70*(5), 1023–1037.
Hooker, S. B., et al. (2012), The fifth SeaWiFS HPLC analysis round-robin experiment (SeaHARRE-5), NASA Technical Memorandum, 217503.
Jickells, T. D., Z. An, K. K. Andersen, A. R. Baker, G. Bergametti, N. Brooks, J. Cao, P. W. Boyd, R. A. Duce, and K. A. Hunter (2005), Global iron connections between desert dust, ocean biogeochemistry, and climate, *Science*, *308*(5718), 67–71.
Kamykowski, D., S. J. Zentara, J. M. Morrison, and A. C. Switzer (2002), Dynamic global patterns of nitrate, phosphate, silicate, and iron availability and phytoplankton community composition from remote sensing data, *Global Biogeochem. Cycles*, *16*(4), 1077, doi:10.1029/2001GB001640.
Karageorgis, A. P., W. D. Gardner, D. Georgopoulos, A. V. Mishonov, E. Krasakopoulou, and C. Anagnostou (2008), Particle dynamics in the Eastern Mediterranean Sea: A synthesis based on light transmission, PMC, and POC archives (1991–2001), *Deep Sea Res., Part I*, *55*(2), 177–202.
Karl, D., R. Letelier, L. Tupas, J. Dore, J. Christian, and D. Hebel (1997), The role of nitrogen fixation in biogeochemical cycling in the subtropical North Pacific Ocean, *Nature*, *388*, 533–538.
Karl, D., A. Michaels, B. Bergman, D. Capone, E. Carpenter, R. Letelier, F. Lipschultz, H. Paerl, D. Sigman, and L. Stal (2002), Dinitrogen fixation in the world's oceans, *Biogeochemistry*, *57*(1), 47–98.
Kérouel, R., and A. Aminot (1997), Fluorometric determination of ammonia in sea and estuarine waters by direct segmented flow analysis, *Mar. Chem.*, *57*(3–4), 265–275.
King, F. D., and A. H. Devol (1979), Estimates of vertical eddy diffusion through the thermocline from phytoplankton nitrate assimilation rates in the mixed layer of the eastern tropical Pacific, *Limnol. Oceanogr.*, *24*(4), 645–651.
Knap, A., A. Michaels, A. Close, H. Ducklow, and A. Dickson (1996), Protocols for the Joint Global Ocean Flux Study (JGOFS) core measurements JGOFS Rep. 19, in Reprint of the IOC Manuals and Guides No. 29, UNESCO, 1994, UNESCO.

Lehodey, P., I. Senina, J. Sibert, L. Bopp, B. Calmettes, J. Hampton, and R. Murtugudde (2010), Preliminary forecasts of Pacific bigeye tuna population trends under the A2 IPCC scenario, *Prog. Oceanogr.*, *86*(1–2), 302–315.
Lewis, M. R., W. G. Harrison, N. S. Oakey, D. Herbert, and T. Platt (1986), Vertical nitrate fluxes in the oligotrophic ocean, *Science*, *234*(4778), 870–872.
Lourey, M. J., J. R. Dunn, and J. Waring (2006), A mixed-layer nutrient climatology of Leeuwin Current and Western Australian shelf waters: Seasonal nutrient dynamics and biomass, *J. Mar. Syst.*, *59*, 25–51.
Mahaffey, C., R. G. Williams, G. A. Wolff, and W. T. Anderson (2004), Physical supply of nitrogen to phytoplankton in the Atlantic Ocean, *Global Biogeochem. Cycles*, *18*, GB1034, doi:10.1029/2003GB002129.
McGillicuddy, D. J., and A. R. Robinson (1998), Interaction between the oceanic mesoscale and the surface mixed layer, *Dyn. Atmos. Oceans*, *27*, 549–574.
McGowan, H., and A. Clark (2008), Identification of dust transport pathways from Lake Eyre, Australia using Hysplit, *Atmos. Environ.*, *42*(29), 6915–6925.
McInnes, A. S., A. K. Shepard, E. J. Raes, A. M. Waite, and A. Quigg (2014), Simultaneous quantification of active carbon-and nitrogen-fixing communities and estimation of fixation rates using fluorescence in situ hybridization and flow cytometry, *Appl. Environ. Microbiol.*, *80*, 6750–6759.
Mohr, W., T. Großkopf, D. W. R. Wallace, and J. LaRoche (2010), Methodological underestimation of oceanic nitrogen fixation rates, *PLoS One*, *5*(9), e12583, doi:10.1371/journal.pone.0012583.
Moisander, P. H., R. A. Beinart, I. Hewson, A. E. White, K. S. Johnson, C. A. Carlson, J. P. Montoya, and J. P. Zehr (2010), Unicellular cyanobacterial distributions broaden the oceanic N_2 fixation domain, *Science*, *327*(5972), 1512–1514.
Monteiro, F. M., M. J. Follows, and S. Dutkiewicz (2010), Distribution of diverse nitrogen fixers in the global ocean, *Global Biogeochem. Cycles*, *24*, GB3017, doi:10.1029/2009GB003731.
Monteiro, F. M., S. Dutkiewicz, and M. J. Follows (2011), Biogeographical controls on the marine nitrogen fixers, *Global Biogeochem. Cycles*, *25*, GB2003, doi:10.1029/2010GB003902.
Montes-Hugo, M., S. C. Doney, H. W. Ducklow, W. Fraser, D. Martinson, S. E. Stammerjohn, and O. Schofield (2009), Recent changes in phytoplankton communities associated with rapid regional climate change along the western Antarctic Peninsula, *Science*, *323*(5920), 1470–1473.
Montoya, J. P., M. Voss, P. Kahler, and D. G. Capone (1996), A simple, high-precision, high-sensitivity tracer assay for N (inf2) fixation, *Appl. Environ. Microbiol.*, *62*(3), 986–993.
Montoya, J. P., C. M. Holl, J. P. Zehr, A. Hansen, T. A. Villareal, and D. G. Capone (2004), High rates of N_2 fixation by unicellular diazotrophs in the oligotrophic Pacific Ocean, *Nature*, *430*(7003), 1027–1032.
Moore, J. K., and S. C. Doney (2007), Iron availability limits the ocean nitrogen inventory stabilizing feedbacks between marine denitrification and nitrogen fixation, *Global Biogeochem. Cycles*, *21*, GB2001, doi:10.1029/2006GB002762.
Morris, R. C., and E. R. Ramanaidou (2007), Genesis of the channel iron deposits (CID) of the Pilbara region, Western Australia, *Aust. J. Earth Sci.*, *54*(5), 733–756.
Mourino-Carballido, B., R. Graña, A. Fernández, A. Bode, M. Varela, J. F. Domínguez, J. Escánez, D. de Armas, and E. Marañón (2011), Importance of N_2 fixation vs. nitrate eddy diffusion along a latitudinal transect in the Atlantic Ocean, *Limnol. Oceanogr.*, *56*, 999–1007.
Murphy, J., and J. P. Riley (1962), A modified single solution method for the determination of phosphate in natural waters, *Anal. Chim. Acta*, *27*, 31–36.
Oschlies, A. (2002), Nutrient supply to the surface waters of the North Atlantic: A model study, *J. Geophys. Res.*, *107*(C5), 3046, doi:10.1029/2000JC000275.
Oschlies, A., and V. Garçon (1998), Eddy-induced enhancement of primary production in a model of the North Atlantic Ocean, *Nature*, *394*, 266–269.
Painter, S. C., M. D. Patey, A. Forryan, and S. Torres-Valdes (2013), Evaluating the balance between vertical diffusive nitrate supply and nitrogen fixation with reference to nitrate assimilation in the eastern subtropical North Atlantic Ocean, *J. Geophys. Res. Oceans*, *118*, 5732–5749, doi:10.1002/jgrc.20416.
Parsons, T. R., Y. Maita, and C. Lalli (1984), *Manual of Chemical and Biological Methods for Seawater Analysis*, Pergamon Press, Oxford.
Paterson, H. L., M. Feng, A. M. Waite, D. Gomis, L. E. Beckley, D. Holliday, and P. A. Thompson (2008), Physical and chemical signatures of a developing anticyclonic eddy in the Leeuwin Current, eastern Indian Ocean, *J. Geophys. Res.*, *113*, C07049, doi:10.1029/2007JC004707.
Paul, D., G. Skrzypek, and I. Fórizs (2007), Normalization of measured stable isotopic compositions to isotope reference scales—A review, *Rapid Commun. Mass Spectrom.*, *21*, 3006–3014.
Pearce, A., and C. B. Pattiaratchi (1999), The Capes Current: A summer countercurrent flowing past Cape Leeuwin and Cape Naturaliste, Western Australia, *Cont. Shelf Res.*, *19*(3), 401–420.
Pearce, A., and M. Feng (2007), Observations of warming on the Western Australian continental shelf, *Mar. Freshwater Res.*, *58*, 914–920.
Planas, D., S. Agusti, C. M. Duarte, T. C. Granata, and M. Merino (1999), Nitrate assimilation and diffusive nitrate supply in the Central Atlantic, *Limnol. Oceanogr.*, *44*(1), 116–126.
Polovina, J. J., E. A. Howell, and M. Abecassis (2008), Ocean's least productive waters are expanding, *Geophys. Res. Lett.*, *35*, L03618, doi:10.1029/2007GL031745.
R Development Core Team (2013), *R: A Language and Environment for Statistical Computing*, R Foundation for Statistical Computing, Vienna, Austria.
Raes, E. J., A. M. Waite, A. S. McInnes, H. Olsen, H. M. Nguyen, N. Hardman-Mountford, and P. A. Thompson (2014), Changes in latitude and dominant diazotrophic community alter N_2 fixation, *Mar. Ecol. Prog. Ser.*, *516*, 85–102, doi:10.3354/meps11009.
Redfield, A. C. (1958), The biological control of chemical factors in the environment, *Am. Sci.*, *46*(3), 205–221.
Rochford, D. (1969), Seasonal variations in the Indian Ocean along 110 EI Hydrological structure of the upper 500 m, *Mar. Freshwater Res.*, *20*(1), 1–50.
Rubin, M., I. Berman-Frank, and Y. Shaked (2011), Dust- and mineral-iron utilization by the marine dinitrogen-fixer Trichodesmium, *Nat. Geosci.*, *4*(8), 529–534.
Ryabenko, E., et al. (2012), Contrasting biogeochemistry of nitrogen in the Atlantic and Pacific Oxygen Minimum Zones, *Biogeosciences*, *9*, 203–215.
Séférian, R., L. Bopp, M. Gehlen, D. Swingedouw, J. Mignot, E. Guilyardi, and J. Servonnat (2014), Multiyear predictability of tropical marine productivity, *Proc. Natl. Acad. Sci. U.S.A.*, *111*(32), 11,646–11,651.
Skrzypek, G., R. Sadler, and D. Paul (2010), Error propagation in normalization of stable isotope data: A Monte Carlo analysis, *Rapid Commun. Mass Spectrom.*, *24*, 2697–2705.

Talley, L. D. (2013), *Volume 4: Indian Ocean*, Intl. WOCE Project Office, Southampton, U. K.
Thompson, P., K. Wild-Allen, M. Lourey, C. Rousseaux, A. Waite, M. Feng, and L. Beckley (2011), Nutrients in an oligotrophic boundary current: Evidence of a new role for the Leeuwin Current, *Prog. Oceanogr.*, *91*(4), 345–359.
Torres-Valdés, S., V. M. Roussenov, R. Sanders, S. Reynolds, X. Pan, R. Mather, A. Landolfi, G. A. Wolff, E. P. Achterberg, and R. G. Williams (2009), Distribution of dissolved organic nutrients and their effect on export production over the Atlantic Ocean, *Global Biogeochem. Cycles*, *23*, GB4019, doi:10.1029/2008GB003389.
Twomey, L., A. Waite, V. Pez, and C. Pattiaratchi (2007), Variability in nitrogen assimilation and fixation in the oligotrophic waters off the south west coast of Australia, *Deep Sea Res., Part II Topical Stud. Oceanogr.*, *54*(8–10), 925–942.
Valsala, V., S. Maksyutov, and R. Murtugudde (2012), A window for carbon assimilation in the southern subtropical Indian Ocean, *Geophys. Res. Lett.*, *39*, L17605, doi:10.1029/2012GL052857.
Verdugo, P., A. Alldredge, F. Azam, D. Kirchman, U. Passow, and P. Santschi (2004), The oceanic gel phase: A bridge in the DOM–POM continuum, *Mar. Chem.*, *92*, 67–85.
Vidussi, F., H. Claustre, B. B. Manca, A. Luchetta, and J.-C. Marty (2001), Phytoplankton pigment distribution in relation to upper thermocline circulation in the eastern Mediterranean Sea during winter, *J. Geophys. Res.*, *106*(C9), 19,939–19,956, doi:10.1029/1999JC000308.
Waite, A. M., S. Pesant, D. A. Griffin, P. A. Thompson, and C. M. Holl (2007a), Oceanography, primary production and dissolved inorganic nitrogen assimilation in two Leeuwin Current eddies, *Deep Sea Res., Part II Topical Stud. Oceanogr.*, *54*(8–10), 981–1002.
Waite, A. M., P. A. Thompson, S. Pesant, M. Feng, L. E. Beckley, C. M. Domingues, D. Gaughan, C. E. Hanson, C. M. Holl, and T. Koslow (2007b), The Leeuwin Current and its eddies: An introductory overview, *Deep Sea Res., Part II Topical Stud. Oceanogr.*, *54*(8–10), 789–796.
Waite, A. M., V. Rossi, M. Roughan, B. Tilbrook, P. A. Thompson, M. Feng, A. S. J. Wyatt, and E. J. Raes (2013), Formation and maintenance of high-nitrate, low pH layers in the eastern Indian Ocean and the role of nitrogen fixation, *Biogeosciences*, *10*(8), 5691–5702.
Waite, A. M., L. E. Beckley, L. Guidi, J. Landrum, D. Holliday, J. Montoya, H. Paterson, M. Feng, P. A. Thompson, and E. J. Raes (2015), Cross-shelf transport, oxygen depletion and nitrate release within a forming mesoscale eddy in the eastern Indian Ocean, *Limnol. Oceanogr.*, in press.
Ward, B., K. Kilpatrick, E. Renger, and R. Eppley (1989), Biological nitrogen cycling in the nitracline, *Limnol. Oceanogr.*, *34*, 493–513.
Ward, B., M. Voss, H. W. Bange, J. W. Dippner, J. J. Middelburg, and J. P. Montoya (2013), The marine nitrogen cycle: Recent discoveries, uncertainties, *Philos. Trans. R. Soc. B Biol. Sci.*, *368*, doi:10.1098/rstb.2013.0121.
Watson, C., N. White, R. Coleman, J. Church, P. Morgan, and R. Govind (2004), TOPEX/Poseidon and Jason-1: Absolute calibration in Bass Strait, Australia, *Mar. Geod.*, *27*(1–2), 107–131.
Weber, T., and C. Deutsch (2014), Local versus basin-scale limitation of marine nitrogen fixation, *Proc. Natl. Acad. Sci. U.S.A.*, *111*, 8741–8746, doi:10.1073/pnas.1317193111.
White, A. E. (2012), Oceanography: The trouble with the bubble, *Nature*, *488*(7411), 290–291.
Williams, R. G., and M. J. Follows (1998), The Ekman transfer of nutrients and maintenance of new production over the North Atlantic, *Deep Sea Res., Part I*, *45*, 461–489.
Williams, R. G., V. Roussenov, and M. J. Follows (2006), Nutrient streams and their induction into the mixed layer, *Global Biogeochem. Cycles*, *20*, GB1016, doi:10.1029/2005GB002586.
Winkler, L. W. (1888), Die Bestimmung des im Wasser gelösten Sauerstoffes, *Ber. Dtsch. Chem. Ges.*, *21*(2), 2843–2854.
Woo, M., and C. Pattiaratchi (2008), Hydrography and water masses off the western Australian coast, *Deep Sea Res., Part I*, *55*(9), 1090–1104.
Yool, A., A. P. Martin, C. Fernández, and D. R. Clark (2007), The significance of nitrification for oceanic new production, *Nature*, *447*(7147), 999–1002.